



## Numerical simulation of concrete hollow bricks by the finite volume method

Jiapeng Sun<sup>a</sup>, Liang Fang<sup>a,b,\*</sup>

<sup>a</sup>School of Materials Science and Engineering, China University of Mining & Technology, Xuzhou 221116, Jiangsu Province, PR China

<sup>b</sup>School of Mechanical & Electrical Engineering, China University of Mining & Technology, Xuzhou 221116, Jiangsu Province, PR China

### ARTICLE INFO

#### Article history:

Received 22 December 2008

Received in revised form 23 May 2009

Accepted 12 June 2009

Available online 27 July 2009

#### Keywords:

Concrete hollow brick

Finite volume method

Equivalent thermal conductivity

Multi-mode heat transfer

### ABSTRACT

Numerical thermal analysis has become a powerful tool for hollow brick design concerning energy saving issue. In the present paper it was employed to understand the heat transfer performance of  $240 \times 115 \times 90$  concrete hollow bricks with 71 different configurations. The general commercial computational fluid dynamics (CFD) soft FLUENT<sup>®</sup> was used in the research. A comprehensive investigation on the effect of enclosure configurations with the same void volume fraction on equivalent thermal conductivity (ETC) was conducted. The enclosure numbers in parallel and vertical directions of heat transfer were investigated in details. The effect of enclosure staggered form is also discussed carefully. In the research, ETC data was compared with radiation and nature convection and without them. In addition, temperature and velocity vector distributions were also illustrated in order to clarify heat transfer mechanism. It can be concluded from this research that ETC values are dependent on the combining effect of heat conduction in all domains, natural convection within enclosure and radiation on inner surface. ETC values decrease with the increasing enclosure numbers in the parallel direction of heat transfer and increase in the vertical direction of heat transfer, vice versa. Therefore, increasing enclosure numbers in the parallel direction becomes more favorable to decrease ETC than that in the vertical direction of heat transfer. Secondly, the relative enhancement of radiation heat transfer on ETC ranged from 7.41% to 25.39%, and the nature convection from near zero to 22.50%, depending on the enclosure numbers and their arrangement configurations. Finally, the increasing enclosures in the parallel direction can decrease ETC values from 11.59% to 20.94% for enclosure vertical aligned bricks. Under the given conditions the smallest ETC is  $0.32619 \text{ W}/(\text{m K})$  for enclosure staggered form with three enclosures in length direction and eight in width direction, which is only 23.30% of the solid concrete brick in the present research.

© 2009 Elsevier Ltd. All rights reserved.

### 1. Introduction

In the worldwide energy crisis, energy saving has become a focusing cared topic by every county over the world. Energy consumption of buildings usually takes up 30–40% of the human's livelihood energy consumption. Many countries choose the building energy saving as a crucial policy. An important part of building energy saving comes from brick material types and its structures. Many researches are, therefore, carried out to obtain the new brick materials with well energy savings.

The concrete hollow brick is widely applied to construct wall replacing the clay brick, as a result of many advantages, such as, soil saving, energy saving, high strength, easy manufacturing and extending material types. However, decreasing heat conductivity for those hollow bricks is the most prior topic. The concrete's conductivity ( $1.40 \text{ W}/(\text{m K})$ ) is approximately two times

than clay that restricts the energy saving efficiency for concrete hollow brick. Many works [1,2,11–16] have indicated that changing the enclosure configuration in the brick or block will extend the original routes for heat flow and will greatly affect the equivalent thermal conductivity (ETC), thus improving their heat insulation properties.

Nowadays many researches are concentrated on the computation of heat transfer process and the influence of parameters of the concrete hollow brick on heat transfer to obtain a satisfied configuration with small ETC, so as us. The heat transfer in concrete hollow brick is a well-known classical multi-mode heat transfer, which consists of heat conduction in all domains, nature convection in enclosures and radiation inner surface. Generally speaking, experimental process can be a good choice for the research, but it becomes tedious with high cost and exhausted durations. Considering numerical simulation, it is a classical computation process of coupling heat transfer. More and more researchers prefer to use numerical simulation to solve the optimization of the hollow brick configuration at present.

During the past two decades, several experimental results and numerical calculations have been presented for describing two-

\* Corresponding author. Address: School of Materials Science and Engineering, China University of Mining & Technology, Xuzhou 221116, Jiangsu Province, PR China.

E-mail address: [fangl@cumt.edu.cn](mailto:fangl@cumt.edu.cn) (L. Fang).

## Nomenclature

$A_{w1}$	area of inner surface ( $m^2$ )	$W$	length of calculation unit in $y$ direction (m)
$A_{w2}$	area of outer surface ( $m^2$ )	$x, y, z$	coordinate (m)
$C$	specific heat of air ( $J/(kg\ K)$ )		
$h_1$	convection heat transfer coefficient of inner surface of wall ( $W/(m^2\ K)$ )	<i>Greek letters</i>	
$h_2$	convection heat transfer coefficient of outer surface of wall ( $W/(m^2\ K)$ )	$\alpha$	the absorption coefficient of air
$H$	length of calculation unit in $z$ direction (m)	$\beta$	volumetric thermal expansion coefficient ( $K^{-1}$ )
$L$	length of calculation unit in $x$ direction (m)	$\varepsilon$	emissivity of the concrete ( $m^{-1}$ )
$Pr$	Prandtl number	$\lambda_{total}$	equivalent thermal conductivity with conduction, nature convection and radiation ( $W/(m\ K)$ )
$q_1$	heat flux through the inner surface ( $W/m^2$ )	$\lambda_{cond}$	mono equivalent thermal conductivity with pure conduction ( $W/(m\ K)$ )
$q_2$	heat flux through the outer surface ( $W/m^2$ )	$\lambda_{cond-conv}$	equivalent thermal conductivity with conduction and nature convection ( $W/(m\ K)$ )
$T$	temperature (K)	$\lambda_{conv}$	mono equivalent thermal conductivity with pure nature convection ( $W/(m\ K)$ )
$T_c$	reference temperature (K)	$\lambda_f$	conductivity of air ( $W/(m\ K)$ )
$T_{f1}$	indoor temperature (K)	$\lambda_{rad}$	mono equivalent thermal conductivity with pure radiation ( $W/(m\ K)$ )
$T_{f2}$	environment temperature (K)	$\lambda_{sta}$	equivalent thermal conductivity of the brick with staggered form enclosure ( $W/(m\ K)$ )
$T_{w1}$	are-weight facet average of the temperature on inner surface (K)	$\bar{\lambda}$	equivalent thermal conductivity ( $W/(m\ K)$ )
$T_{w2}$	are-weight facet average of the temperature on outer surface (K)	$\mu$	dynamic viscosity ( $kg/m\ s$ )
$u$	velocity component in $x$ direction (m/s)	$\rho_c$	reference density of the air ( $kg/m^3$ )
$v$	velocity component in $y$ direction (m/s)	$\rho_f$	density of the air ( $kg/m^3$ )
$w$	velocity component in $z$ direction (m/s)		

dimensional multi-mode heat transfer of hollow bricks with single enclosure. Most interests are involved in heat transfer with different Rayleigh numbers, aspect ratios and tilted angles. Heat conduction and surface radiation of brick wall with natural convection have been discussed in a two-dimensional rectangular cavity by Kim and Viskanta [3,4]. They performed experimental and numerical studies on a square cavity having four walls with finite thickness. It has been concluded that natural convection in the cavity can be reduced by coupled action from heat conduction in the walls and radiation exchange among surfaces. Ren et al. [5] studied the combined heat transfer in enclosure with the radiation and nature convection. They have indicated that the radiation can take up about 30% of heat energy. Recently, Hinojosa et al. [6] predicted the Nusselt number for the natural convection and surface thermal radiation in a square tilted open cavity. They have got that the heat transfer via radiation is in the same order of natural convection. Misra [7] studied conjugate conduction with nature convection in a square enclosure with a conducting vertical wall by FEM. It has been concluded that the conductivity-to-wall thickness is the determining factor for prediction of Nusselt number. Mobedi [8] studied conjugate natural convection in square cavity with finite thickness horizontal walls. It has been found that although the horizontal walls do not directly reduce temperature difference between the vertical walls of cavity, heat transfer rate across the cavity is decreased particularly for large ratio of Rayleigh number and thermal conductivity.

In recent decade, some 2D numerical calculations have been conducted for predicting the heat transfer performance of the hollow brick. 2D simulation of enclosures has been conducted to the hollow clay bricks with single or double enclosures by Zhao [9]. In that research surface radiation is taken into account by treating the radiation energy as the additional source term of the control volume bounded with the surface. The results emphasized the effect of the thermal boundary condition on the total heat transfer. Majed [10] studied the coupled natural convection effects on the heat transfer using commercial software FLUENT®. Three different configurations of building bricks are considered. The first is a typ-

ical brick with three identical hollow cells (air cavities), the second obtained by filling these cells with ordinary polystyrene bars and the third obtained by using hollow polystyrene bars. It has been concluded that the second can reduce the heat transfer rate by 36%, compared with the first. The third can only reduce only by 6% due to the air motion inside the enclosures in the polystyrene bars. Most work above mentioned is concerned with two-dimensional modeling.

Recently, some 3D numerical thermal simulations are conducted. All those reports focus on the effect of the specific configuration on the heat-insulating property of the hollow brick using the parameter of the equivalent thermal conduction (abbreviate to ETC) or the mass overall thermal efficiency. In those simulations, the computational domains consist of several hollow bricks. The simulation results give out the heat-insulating property of the overall wall in nature. However, very few papers involve the effect on the multi-mode heat transfer process and heat-insulating property of the configuration of the hollow brick. del Coz Díaz [11–14] conducted a 3D simulation about some kinds of light concrete hollow brick walls and light concrete multi-holed bricks by finite element method. In their work the nature convection and radiation are considered as boundary condition and the parameter of mass overall thermal efficiency was used to evaluate the economic efficiency of the concrete hollow brick. Li [15] has carried out the simulation of  $290 \times 140 \times 90$  hollow clay bricks for 72 kinds of different enclosure configurations. The optimum configuration is got, which should be a structure with eight enclosures in length, four enclosures in width and one communicating enclosure in height and the brick is with the lowest ETC  $0.400\ W/(m\ K)$ , which is only 59% of the highest thermal conductivity of the all cases studied. In their work enclosure volume fractions are varied which has flawed applied to evaluate ETC of the brick enclosure configuration. Besides, in order to examine the contributions of conduction, convection and radiation to ETC, respectively, the influence of above three heat transfer components on ETC has not yet been separately discussed. Li's [16] another paper on multi-holed clay bricks with the size of  $240 \times 115 \times 90$  shows the similar results.

The optimum configuration has five length-wise holes and four width-wise holes with ETC 0.419 W/(m K), which is only 53.1% of solid clay.

Overall, the numerical thermal simulation is successfully applied to the multi-model heat transfer computation of hollow brick or block, and has obtained some satisfied results. However, the systemic study on the effect of enclosure configurations and multi-model heat transfer process, especially on the relative fractions of the conductivity, nature convection and radiation, are not easily found in literatures. This is just the present research content. The study is significant for understanding the heat transfer characteristic, more improving the heat insulation property of concrete hollow brick and designing the new concrete hollow brick. The result can also be used to simplify the mathematical optimization model in order to obtain the optimum concrete hollow brick.

In the present paper, the ETC is calculated for 71 kinds of 240 mm(length) × 115 mm (width) × 90 mm (height) hollow bricks which is widely applied in the present building constructions of China. The general commercial CFD (abbreviation for computational fluid dynamics) soft FLUENT<sup>®</sup> is used in the research. A comprehensive investigation on the effect of enclosure configurations with the same void volume fraction on ETC is conducted to understand the contributions of every heat transfer component, such as, conductivity, nature convection and radiation to ETC, the values of every heat transfer component are also estimated besides ETC. Finally, the effect of enclosure staggered form on heat transfer is also discussed carefully. As mentioned above, the heat transfer in hollow brick is a multi-mode heat transfer process which contains conduction in all domains, nature convection in enclosures, and radiation on inner surface. Different configuration of the hollow brick affects the relative fractions of conduction, convection and surface radiation in the heat transfer process. Theoretically, the heat transfer process in the hollow brick is unsteady because either outdoor or indoor environment varies from time to time and the outdoor radiation varies too. However, from engineering point of view, a steady state assumption can be applied to simplify the simulation process. Therefore, typical indoor and outdoor temperatures are required to be pre-defined. Here outdoor radiation is assumed as affixed temperature which is equivalent to increased outdoor air temperature. The affixed temperature is calculated in the present research using the China Standard for Design of Heating Ventilation and Air Conditioning (GB50019-2003.)

## 2. Mathematical modeling

Fig. 1 shows a typical configuration of 240 × 115 × 90 concrete hollow brick, which is commonly used in China, with 0.24 m in length, 0.115 m in width, 0.09 m in height.

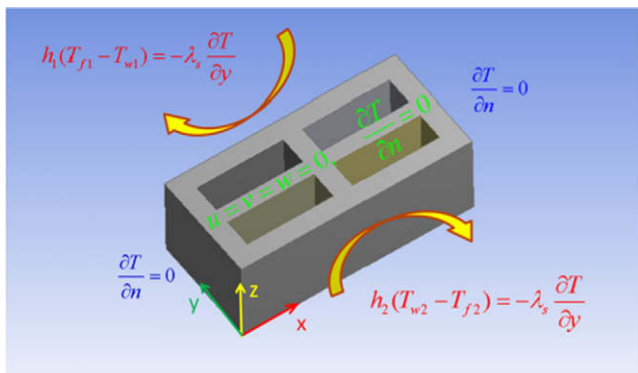


Fig. 1. Schematic diagram of geometry and the computation model.

In maintaining a constant void volume fraction of 37.80%, the effect of enclosure number in both length and width directions on ETC are discussed below. Enclosure numbers in both the length and width directions of the brick is, therefore, varied in purpose. Either in the length or the width direction, the number of enclosures is changed from 1 to 8, individually. The enclosures in the same concrete hollow brick have the same exterior size. So, 64 types of 240 × 115 × 90 concrete hollow bricks with different enclosures and arrangements are obtained for the simulation. To be convenient the concrete hollow brick with n1 enclosures in length direction and n2 enclosures in width direction is denoted as Bn1-n2. For example, the concrete hollow brick as shown in Fig. 1 is indicated as B2-2. ETC of bricks is simulated by changing the number of the enclosures in one direction and keeping a constant number in another direction. It has been reported [17] that the enclosure staggering form can decrease ETC effectively. In the present research it is also discussed.

In the simulation process the thermal physical properties of the concrete and air are assumed as constants. The density of the concrete skeleton material is 2200 kg/cm<sup>3</sup> and the conductivity is 1.40 W/(m K).

Air in the hollow brick is considered as incompressible in steady laminar state. The Boussinesq assumption [18] is held in the simulation which means neglecting viscous dissipation in liquid. All the properties of matter are assumed constant except density which is taken as variable parameter of body force in momentum equation.

$$\rho = \rho_c [1 - \beta(T - T_c)] \quad (1)$$

where  $T_c$  is the reference temperature of cold surface.  $\rho_c$  the liquid density correspond to  $T_c$  and  $\beta$  the coefficient of body expansion.

The governing equations related to mass, momentum and energy equations can be stated as follows:

For solid wall

Conduction equation:

$$\frac{\partial}{\partial x} \left( \lambda \frac{\partial T}{\partial x} \right) + \frac{\partial}{\partial y} \left( \lambda \frac{\partial T}{\partial y} \right) + \frac{\partial}{\partial z} \left( \lambda \frac{\partial T}{\partial z} \right) = 0 \quad (2)$$

Inside the air filled enclosures

Continuity equation:

$$\frac{\partial u}{\partial x} + \frac{\partial v}{\partial y} + \frac{\partial w}{\partial z} = 0 \quad (3)$$

Momentum in x-direction:

$$\rho \left( u \frac{\partial u}{\partial x} + v \frac{\partial u}{\partial y} + w \frac{\partial u}{\partial z} \right) = -\frac{\partial p}{\partial x} + \mu \left( \frac{\partial^2 u}{\partial x^2} + \frac{\partial^2 u}{\partial y^2} + \frac{\partial^2 u}{\partial z^2} \right) \quad (4)$$

Momentum in y-direction:

$$\rho \left( u \frac{\partial v}{\partial x} + v \frac{\partial v}{\partial y} + w \frac{\partial v}{\partial z} \right) = -\frac{\partial p}{\partial y} + \mu \left( \frac{\partial^2 v}{\partial x^2} + \frac{\partial^2 v}{\partial y^2} + \frac{\partial^2 v}{\partial z^2} \right) \quad (5)$$

Momentum in z-direction:

$$\rho \left( u \frac{\partial w}{\partial x} + v \frac{\partial w}{\partial y} + w \frac{\partial w}{\partial z} \right) = -\frac{\partial p}{\partial z} + \mu \left( \frac{\partial^2 w}{\partial x^2} + \frac{\partial^2 w}{\partial y^2} + \frac{\partial^2 w}{\partial z^2} \right) + \rho_c g \beta (T - T_c) \quad (6)$$

Energy equation:

$$\frac{\partial T}{\partial \tau} + u \frac{\partial T}{\partial x} + v \frac{\partial T}{\partial y} + w \frac{\partial T}{\partial z} = \alpha \left( \frac{\partial^2 T}{\partial x^2} + \frac{\partial^2 T}{\partial y^2} + \frac{\partial^2 T}{\partial z^2} \right) \quad (7)$$

The boundary conditions are as follows, and are showed in Fig. 1.

$$\begin{aligned}
 y = 0, \quad h_2(T_{w2} - T_{f2}) &= -\lambda_s \frac{\partial T}{\partial y} \\
 y = W, \quad h_1(T_{f1} - T_{w1}) &= -\lambda_s \frac{\partial T}{\partial y} \\
 x = 0, \quad \frac{\partial T}{\partial x} &= 0 \\
 x = L, \quad \frac{\partial T}{\partial x} &= 0 \\
 z = 0, \quad u = v = w = 0, \quad \frac{\partial T}{\partial z} &= 0 \\
 z = H, \quad u = v = w = 0, \quad \frac{\partial T}{\partial z} &= 0
 \end{aligned} \tag{8}$$

where  $L$ ,  $W$  and  $H$  represent the length, width, and height, respectively. The direction of the heat transfer is in the  $y$  direction. So,  $y = 0$  is for outer surface and  $y = W$  for inner surface.

According to the ‘‘Code for design of heating ventilation and air conditioning’’ in China, the indoor temperature should be kept around 18 °C. Indoor convection heat transfer coefficient is 8.70 W/(m<sup>2</sup> K) and outdoor convection heat transfer coefficient 23.00 W/(m<sup>2</sup> K) in heating period of winter season in Xuzhou, Jiangsu Province, China. For outdoor temperature a building energy conservation software DeST-h is used to calculate outdoor composite temperature. The estimated value for outdoor composite temperature in Xuzhou area is –3.4 °C during winter period.

The enclosures’ inner walls are assumed to diffusing surface, and the emissivity  $\varepsilon$  is 0.94 [19]. The air in enclosure is assumed to gray gas. The air’s absorption coefficient  $\alpha$  is 0.01 m<sup>–1</sup>. The scattering is neglected.

The thermal physical properties employed in the simulation are listed in Table 1.

### 3. Numerical simulation approach

#### 3.1. General remarks

The above governing equations are discretized by conventional finite volume method which is adopted by many commercial CFD soft, such as, FLUENT®, CFX® and STAR-CD®, etc. The discretization for momentum and energy term belongs to a second-order difference scheme. In order to obtain a high accuracy pressure staggering option (often abbreviated to PRESTO) [20] is used in pressure calculation and semi-implicit method for pressure-linked equation (often abbreviated to SIMPLE) [20] in pressure–velocity algorithm. The radiation term is solved using the discrete transfer radiation model (often abbreviated to DTRM) [21,22].

#### 3.2. Computing of ETC

In the present research, ETC is got from the simulation to show the thermal insulation characteristic of the concrete hollow brick. According to the heat flux equilibrium condition:

$$q_1 = h_1(T_{f1} - T_{w1}) = q_2 = h_2(T_{w2} - T_{f2}) = \bar{\lambda} (T_{w1} - T_{w2}) \tag{9}$$

Then

$$\bar{\lambda} = W \cdot \frac{q_1}{T_{w1} - T_{w2}} = W \cdot \frac{q_2}{T_{w1} - T_{w2}} \tag{10}$$

In order to decrease the simulating deviation, the mean of  $q_1$  and  $q_2$  is defined for

$$q = \frac{q_1 + q_2}{2} = \frac{h_1(T_{f1} - T_{w1}) + h_2(T_{w2} - T_{f2})}{2} \tag{11}$$

$q_1$  or  $q_2$  in (10) is replaced by  $q$  in (11)

$$\bar{\lambda} = W \cdot \frac{q}{T_{w2} - T_{w1}} = W \cdot \frac{h_1(T_{f1} - T_{w1}) + h_2(T_{w2} - T_{f2})}{2(T_{w1} - T_{w2})} \tag{12}$$

In Eqs (9)–(12), the  $T_{w1}$  and  $T_{w2}$  can be obtained from the simulation, and shown as:

$$\begin{aligned}
 T_{w1} &= \frac{1}{A_{w1}} \sum_{i \in A_{w1}} A(i) * T_w(i) \\
 T_{w2} &= \frac{1}{A_{w2}} \sum_{i \in A_{w2}} A(i) * T_w(i)
 \end{aligned} \tag{13}$$

where  $W$  is the width of the hollow brick,  $T_w(i)$  the temperature of the grid points at the inner and outer surface of the concrete hollow brick and  $A(i)$  the area of the control volume at the inner and outer surface. Above expressions are called are-weight facet average of the temperature.

#### 3.3. Convergence criteria

Convergence criteria of the iteration procedure are as follows

$$R_{ite}/R_{max5} < 10^{-5} \tag{14}$$

and

$$|Q_{in} - Q_{out}| / \min(Q_{in}, Q_{out}) < 10^{-2} \tag{15}$$

In the present computation, the first criterion is easily met. The second criterion is, however, hardly reached. The total number of iterations varies from case to case, ranging from about 500 to 1500.

#### 3.4. Mesh generation and its size estimation

Based on heat transfer theory, the much smaller the enclosure is, the much weaker the nature convection in enclosure is. So, the concrete hollow bricks with large enclosures should have more fine meshes to get accurate results during the simulation. It becomes necessary to check the independency of mesh numbers to simulated accuracy. In the present research a B2-2 brick is used to perform the calculation. Three types hexahedron meshes with different numbers are used to inspect the accuracy of ETC. The first type has the maximum size 0.0015 m in  $x$ – $z$  section and 0.002 m in height direction with the total element numbers 654,515. The second type has the maximum size 0.0012 m in  $x$ – $z$  section, and 0.00225 m in height direction with the total element numbers 916,542. The third type has the same size in  $x$ – $z$  section with the second, but the maximum size 0.0015 m is used in height direction with the total elements numbers 1,316,178. The computational results of ETC are showed in Fig. 2. It is indicated from Fig. 2 that all of them are with little difference. Further calculations show that it only leads to 0.081% errors increasing of the mesh number by two

**Table 1**  
The thermal physical properties using in the simulation.

Property	$T_{f1}$ (K)	$T_{f2}$ (K)	$h_1$ (W/(m <sup>2</sup> K))	$h_2$ (W/(m <sup>2</sup> K))	$P_r$	$\varepsilon$
Value	291.15	269.75	8.70	23.00	0.707	0.94
Property	$C$ (J/(kg K))	$\lambda_f$ (W/(m K))	$\mu$ (kg/(m s))	$\rho_f$ (kg/m <sup>3</sup> )	$\beta$ (K <sup>–1</sup> )	$\alpha$ (m <sup>–1</sup> )
Value	1004.40	0.0261	$1.831 \times 10^{-5}$	1.185	0.003356	0.01

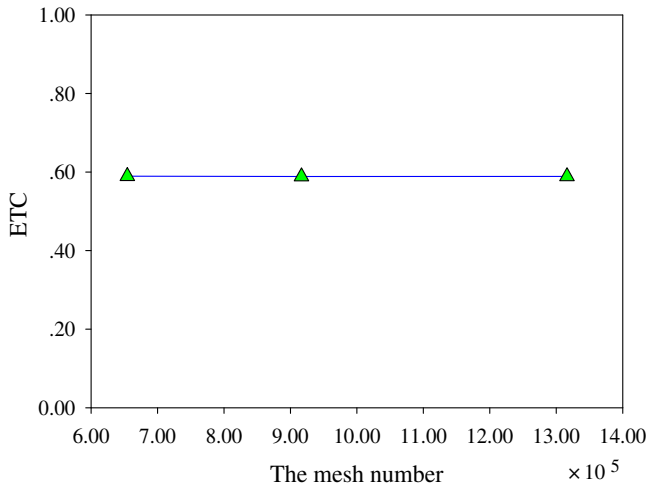


Fig. 2. Mesh-independence check.

times. Therefore, the second type is used in the present research. It is noticed that the wall thickness between enclosures is becoming less and less with the increase of the enclosure numbers. If mesh numbers are chosen comparably rare in one direction of the enclosures, a large calculating error is easily produced.

The simulation is carried out using a personal computer with CPU Core2 E8200, 4 GB RAM memory and 320 GB hard disk.

4. Numerical simulations and results

By changing enclosure numbers in length and width direction, heat transfer model, and arrangement form, ETC of the bricks is calculated and their temperature fields are also simulated by FLU-ENT®. Firstly, radiation and nature convection are both considered to get accurate data. ETC using above simulating strategy is denoted as  $\lambda_{total}$  in following sections. Secondly, the simulations are carried out without considering radiation process to evaluate the

influence of radiation on ETC, which is denoted as  $\lambda_{cond-conv}$  in following sections. Thirdly, the pure conduction simulations are carried out. The resulting ETC is denoted as  $\lambda_{cond}$ . Finally, the simulations are done for staggering arrangement enclosures. The resulting ETC is denoted as  $\lambda_{sta}$  in following sections.

Table 2 shows the simulated ETC for bricks with different enclosure columns and rows in which the rows represent the enclosure numbers in width direction and the columns the enclosure numbers in length direction. There are three rows in every cell in Table 2 in which data in upper row represents  $\lambda_{total}$ , data in bottom row  $\lambda_{cond}$  and data in center row  $\lambda_{cond-conv}$ .

In Table 2, it indicates that the least ETC of the B1-8 concrete hollow brick is just 0.34277 W/(m K), which is 24.29% of ETC for solid concrete hollow brick (1.40 W/m K). So the reasonable assignment of enclosures in the concrete hollow brick can decrease ETC effectively.

4.1. Relationship between ETC and the number of the enclosures in width direction

Fig. 3 shows  $\lambda_{total}$  related to enclosure numbers of the bricks in width direction when air temperature outdoor is  $-3.4\text{ }^\circ\text{C}$  and air temperature indoor  $18\text{ }^\circ\text{C}$ . It can be seen from Fig. 3 that  $\lambda_{total}$  decreases rapidly with the number of enclosures in the width direction and the amplitude decreasing is nonlinear. The change of amplitude becomes intense from one to four enclosures, then, it becomes moderate from five to eight enclosures.

When the ratio of width and height of aperture  $b/h \geq 0.28$ , it can be considered as infinite space natural convection and when  $b/h < 0.28$ , it can be considered as finite space natural convection from heat transfer principle [17]. The hollow brick B1-1 with  $b/h$  0.64, which is greater than 0.28, belongs to the infinite space natural convection. The large spacing in the width-wise direction gives an enough space for fully developed convection. Thus the intensive air convection within the enclosure makes heat transfer be the strongest compared to other bricks with more enclosure numbers. When the enclosure number in width direction is increase to 2, the  $b/h$  decreases to 0.32 which is still larger than

Table 2 The simulated ETC  $\lambda_{total}$  (for upper rows),  $\lambda_{cond-conv}$  (for center rows) and  $\lambda_{cond}$  (for bottom rows).

	1 <sup>a</sup>	2	3	4	5	6	7	8
1 <sup>b</sup>	0.72610	0.74694	0.75457	0.75775	0.75841	0.75781	0.75679	0.75572
	0.54482	0.59466	0.61861	0.63321	0.64309	0.65052	0.65589	0.66038
	0.38147	0.46055	0.49590	0.51432	0.52712	0.53550	0.54225	0.54558
2	0.54632	0.58873	0.60096	0.61062	0.61623	0.61974	0.61284	0.62327
	0.40761	0.46789	0.49393	0.51147	0.52327	0.53179	0.52764	0.54292
	0.35320	0.41631	0.44985	0.47235	0.48790	0.49929	0.49701	0.51549
3	0.45753	0.50096	0.52423	0.53841	0.54818	0.55501	0.56039	0.56492
	0.34618	0.40465	0.43704	0.45713	0.47142	0.48199	0.49046	0.49783
	0.31818	0.38569	0.42247	0.44513	0.46124	0.47331	0.48304	0.49144
4	0.40982	0.45581	0.48159	0.49815	0.50944	0.51812	0.52524	0.54261
	0.31515	0.37325	0.40716	0.42894	0.44397	0.45568	0.46530	0.48600
	0.30786	0.36844	0.40393	0.42649	0.44198	0.45403	0.46391	0.48493
5	0.38306	0.42313	0.45601	0.47311	0.48522	0.49431	0.50185	0.50828
	0.30135	0.35069	0.39158	0.41340	0.42879	0.44037	0.45000	0.45818
	0.29879	0.34921	0.39091	0.41294	0.42844	0.44007	0.44977	0.45799
6	0.36546	0.41092	0.43783	0.45493	0.46702	0.47640	0.48380	0.49028
	0.29403	0.34792	0.38111	0.40237	0.41738	0.42886	0.43809	0.44603
	0.29319	0.34757	0.38078	0.40225	0.41726	0.42875	0.43804	0.44600
7	0.35262	0.39716	0.42415	0.44108	0.45293	0.46262	0.46953	0.47580
	0.28941	0.34098	0.37347	0.39414	0.40861	0.42027	0.42863	0.43619
	0.28915	0.34085	0.37340	0.39408	0.40856	0.42022	0.42860	0.43615
8	0.34277	0.38064	0.41214	0.42947	0.44141	0.45064	0.45775	0.46212
	0.28613	0.32658	0.36628	0.38700	0.40130	0.41219	0.42065	0.42788
	0.28601	0.32646	0.36626	0.38698	0.40127	0.41217	0.42062	0.42582

<sup>a</sup> The enclosure numbers in width direction of hollow brick.  
<sup>b</sup> The enclosure numbers in length direction of hollow brick.



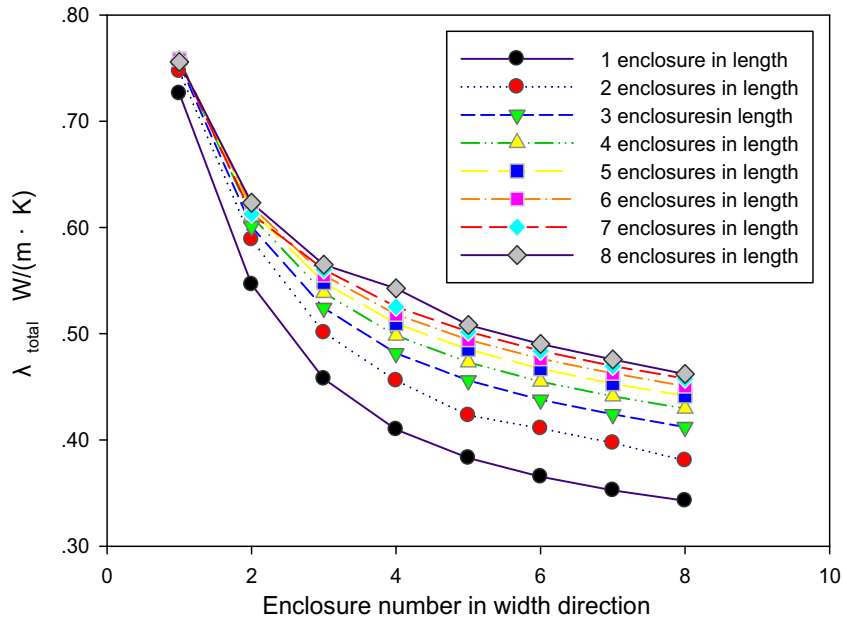


Fig. 3. Effect of enclosure number in width direction on  $\lambda_{total}$ .

0.28. The convection in every enclosure also belongs to infinite convection, but the convection is weaker than that in B1-1 because of the decrease of enclosure size in width direction. In addition, the temperature difference between the two walls decreases in width direction for every enclosure with the increase of enclosure number, resulting in weak convection. The rapidly decreasing tendency lasts to B1-4 hollow brick. When the enclosure number increases further continually, the heat conduction becomes predominant so that the trend becomes leveled off.

As considering the effect of radiation, the process of increasing the number of enclosures in width direction can be explained as such a process that a concrete shield-like plate is inserted to the middle of enclosure. The inserted plate plays a shielding role to

block radiation. Therefore, more enclosure numbers in width direction increase the radiation thermal resistance. In Chapter 5, it can be showed that the conduction also become weak slightly with the increasing enclosure numbers in width. Conduction, nature convection and radiation on inner surface all become weak, which lead to decreasing of ETC  $\lambda_{total}$  with increasing enclosure number in width.

4.2. Relationship between ETC and the number of the enclosures in length direction

Fig. 4 shows  $\lambda_{total}$  related to enclosure numbers in length direction. It indicates that all  $\lambda_{total}$  curves have the similar increase ten-

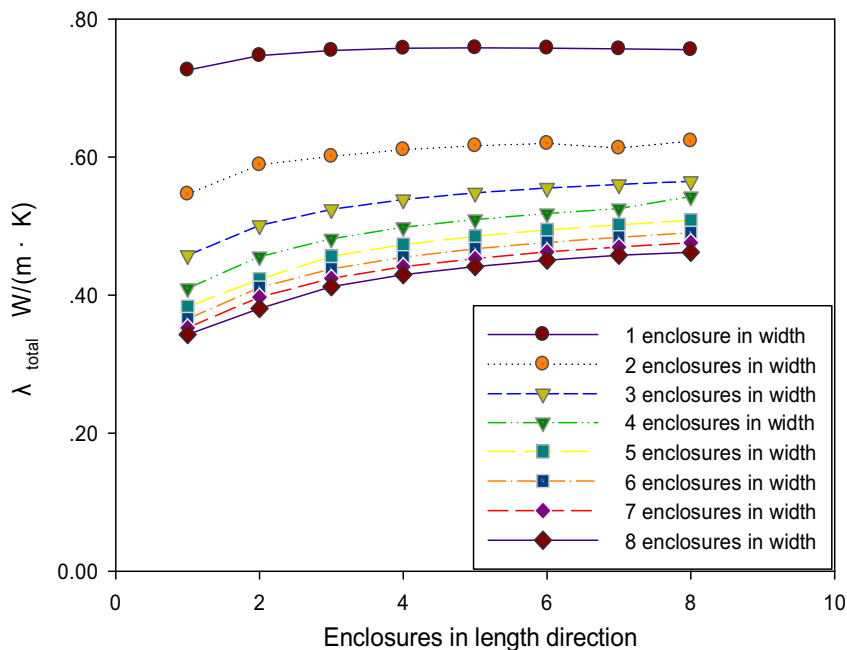


Fig. 4. Effect of enclosure number in length direction on  $\lambda_{total}$ .

dencies with increasing enclosure numbers in length direction and without any intersection for any curve. It is noticed by comparing Figs. 3 and 4 that all curves are leveled off when the enclosure numbers are increased to larger value whatever it is in width direction or in length direction. It is concluded that the enclosure numbers in width and in length direction have coupling effect on ETC. As shown in Table 2, the  $\lambda_{total}$  of seven enclosures brick in width is changed from 0.35262 to 0.47580 when the enclosure number in length varies from one to eight, that is, the  $\lambda_{total}$  is increased 1.35 times while enclosure numbers in length is increased to eight from one. In this case  $\lambda_{total}$  of brick B7-8 becomes the maximum in the series of brick B7-*n*.

Increasing enclosure number in length direction can be explained as such a process that a concrete shield-like plate is inserted to the middle of enclosures. The plate plays different roles in radiation, nature convection and conduction. The influence of the concrete shield on ETC depends on three factors. They are: (1) the effect to resist radiation, (2) the effect to weaken convection and (3) the effect to enhance conduction. Fig. 5 shows the temperature contour of bricks B1-7 and B5-7 at *x* axis plane located at the center of the first rib nearby brick boundary. It can be seen from Fig. 5 that temperature gradient for the brick B5-7 increases compared to that for the brick B1-7, which means the enhancement of conduction heat flux with increasing enclosure numbers in length direction. In following section, the fractions of conduction, convection and radiation related to total ETC will be discussed, respectively. It has been got from related data that conduction becomes a predominant factor to control total ETC. Therefore, total heat flux is increased for brick B5-7, compared to brick B1-7, although radiation and convection are weakened in a way.

4.3. Effect of the enclosure staggered form on ETC

In commercial applications, enclosure staggered form is often applied to obtain a smaller ETC value. Theoretically, the bricks with enclosure staggered form have longer pathways of heat flux than enclosure aligned form, which can increase the thermal resistance.

There are numerous patterns of enclosure staggered forms that can help for the discussion. In the present paper, only one pattern is discussed. Brick B8-8 (see Fig. 6) with enclosure staggered form is simulated. Some half-length enclosures (Fig. 6) are interlaced arrangement in boundaries at the both sides in length direction. The similar arrangements are also configured for brick B2-8, B3-8, B4-8, B5-8, B6-8, and B7-8. They are denoted as brick S2-8, S3-8, S4-8, S5-8, S6-8, S7-8 and S8-8, respectively, to distinguish bricks with aligned enclosures.

ETC of the hollow bricks with enclosure staggered form that is denoted as  $\lambda_{sta}$  is listed in Table 3.  $\lambda_{sta}$  is evidently smaller than

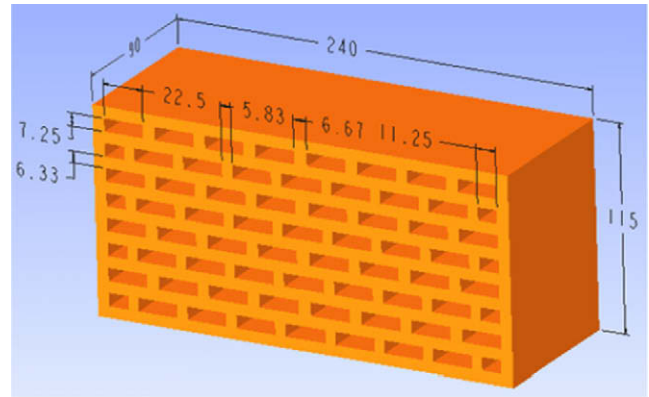


Fig. 6. Schematic of brick S8-8.

$\lambda_{total}$ . The improvement fraction of ETC by enclosure staggered form, that is,  $(\lambda_{total} - \lambda_{sta})/\lambda_{total}$ , is also shown in Table 3. The smallest ETC is 0.32619 W/(m K) which is obtained by brick S3-8. The largest improvement fraction can be 20.94% for brick S4-8 as listed in Table 3. Obviously, the hollow brick with enclosure staggered form is perfect. The smallest ETC is 0.32619 W/(m K) for brick S3-8 which is only 23.30% of the solid concrete brick.

5. Discussion of results

Multi-mode heat transfer in concrete hollow brick contains conduction in all domains, nature convection in enclosures and radiation on inner surface. Different configuration of the hollow brick affects the relative contributions of conduction, convection and radiation in heat transfer process. As discussed in following sections, the effect of the conduction, nature convection and radiation heat transfer on ETC is evaluated by  $\lambda_{cond}$ ,  $\lambda_{conv}$  and  $\lambda_{rad}$ , respectively.  $\lambda_{conv}$  is defined as  $\lambda_{cond-conv} - \lambda_{cond}$  and  $\lambda_{rad}$  as  $\lambda_{total} - \lambda_{cond-conv}$ .  $\lambda_{cond}$ ,  $\lambda_{conv}$  and  $\lambda_{rad}$  are defined as mono-ETC which are related to enclosure number in width and length direction as shown in Fig. 7. Fig. 8 shows  $\lambda_{cond}$ ,  $\lambda_{conv}$  and  $\lambda_{rad}$  related to enclosure number in length direction with the fixed enclosure number 3 in width direction, and Fig. 9 related to enclosure number in width direction with the fixed enclosure number 4 in length direction.

5.1. Effect of radiation on ETC

In Fig. 7, it can be seen that the radiation effect is continuously reduced with increasing enclosure number either in width or length direction. The reason for it is that the increase of enclosure

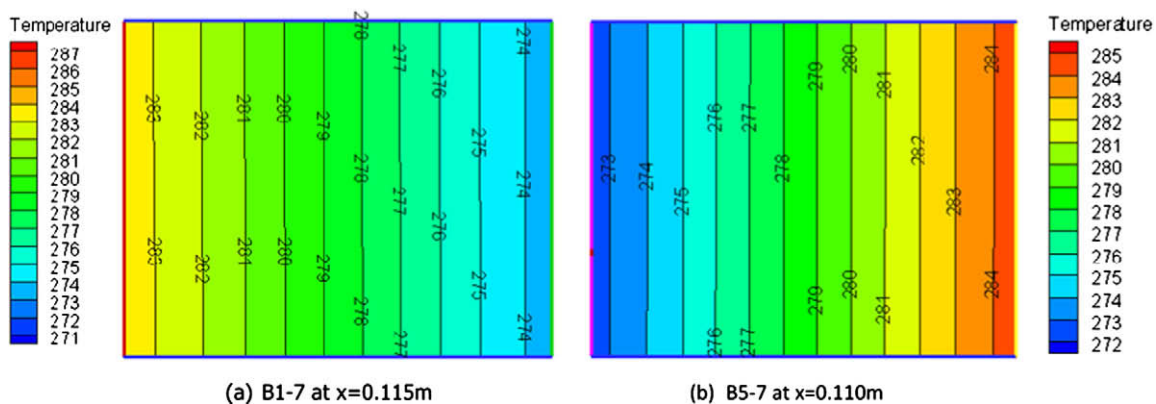


Fig. 5. Temperature contour at the cross-section of concrete shield.

**Table 3**  
The ETC of the hollow brick with the staggered enclosures.

	S2-8	S3-8	S4-8	S5-8	S6-8	S7-8	S8-8
$\lambda_{sta}$	0.33652	0.32619	0.33956	0.35782	0.37632	0.39385	0.41031
$\lambda_{total}$	0.38064	0.41214	0.42947	0.44141	0.45064	0.45775	0.46212
Deviation (%)	11.59	20.86	20.94	18.94	16.49	13.96	11.21

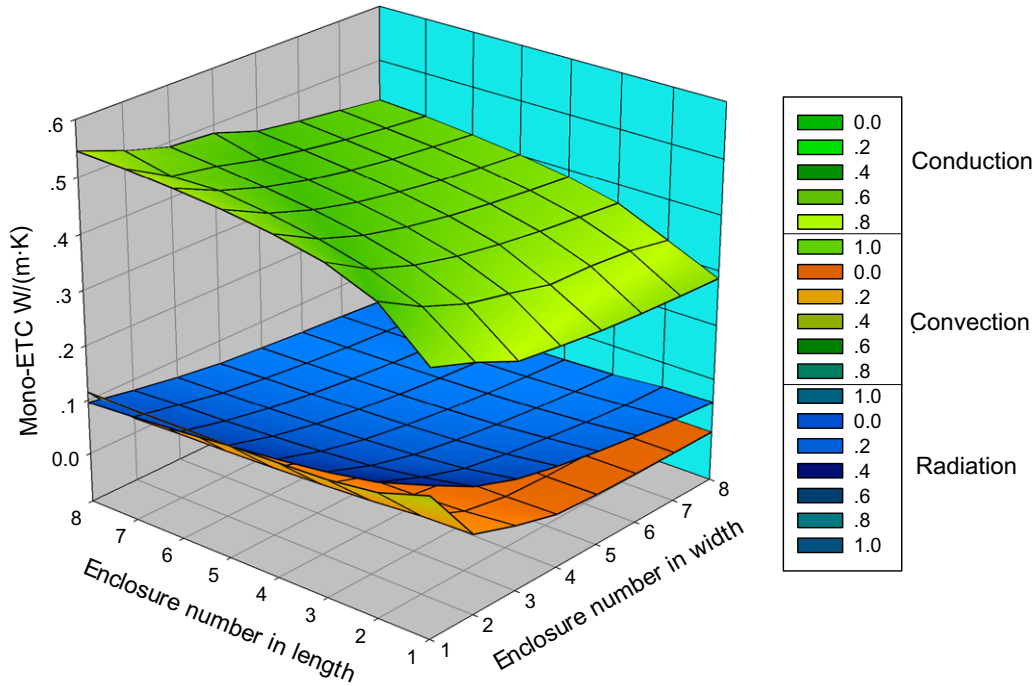


Fig. 7. Three-dimensional mono-ETC surfaces related to enclosure numbers.

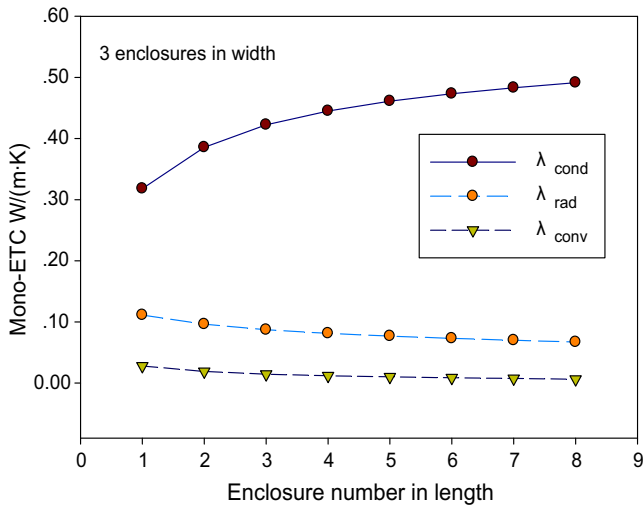


Fig. 8. Mono-ETC for brick with three enclosures in width direction.

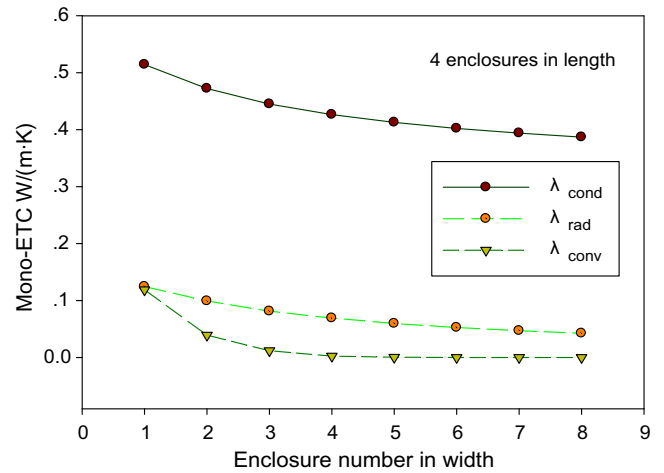


Fig. 9. Mono-ETC for brick with four enclosures in length direction.

number leads to the increase of separated walls between two neighboring enclosures, which are served as radiation shields between the hot and cold surfaces. The minimum mono-ETC is 0.03424 W/(m K) occupying 7.41% of  $\lambda_{total}$  which is found for brick B8-8. The maximum mono-ETC is 0.18128 W/(m K) occupying 24.97% of  $\lambda_{total}$  which is found for brick B1-1.

The parameter  $\lambda_{rad} / \lambda_{total}$  indicates the percentage of the radiation to ETC. It ranges from 7.41% to 25.39%. Although the contribution of the surface radiation to ETC is limited, it will also lead to a

large error if the radiation is ignored with larger enclosures specially. So the radiation should be taken into account in engineering significance.

5.2. Effect of convection on ETC

Similar to above discussed,  $\lambda_{conv}$  is also employed to evaluate the effect of the nature convection on ETC as showed in Figs. 7–9. It indicates that the convection effect rapidly tends to decrease with increasing enclosure numbers in width direction, and moder-



ately decreases with increasing enclosure number in length direction. The former comes from the space limitation to the sufficient development of natural convection. The latter comes from the viscous force between the air and the wall in length direction.

The percentage of  $\lambda_{conv}$  in  $\lambda_{total}$  is ranged from 0.0049% to 22.50%. It will be less than 0.67% when the enclosure number is larger than 5 in width or length direction, and the convection effect can be neglected in engineering significance in this case. Contrary to the radiation, the effect of the convection is weak. So decreasing ETC from the view of the radiation is effective than that of the nature convection.

5.3. Effect of conduction on ETC

From Figs. 7–9, it can be seen that the varying potential of value  $\lambda_{cond}$  is similar to  $\lambda_{total}$  with increasing enclosure number either in width and length, and  $\lambda_{cond}$  is very larger than  $\lambda_{conv}$  and  $\lambda_{rad}$ . The percentage of  $\lambda_{cond}$  in  $\lambda_{total}$  ranges from 52.54% to 98.91%. It shows that the conduction effect is dominant in the present research.

It can be found from Table 2 that the least  $\lambda_{cond}$  is 0.28601 W/(m K). In other words, it is the smallest  $\lambda_{total}$  that can be obtained in the present simulated conditions.

5.4. Multi-mode heat transfer in concrete hollow brick

From above discussion, it can be found that different configuration of the hollow brick affects the relative contributions of conduction, convection and radiation in multi-mode heat transfer process. The conduction effect on ETC is dominant in all configurations. The convection and radiation effect decreases with the increase of the

enclosure number either in width or length. The radiation effect is larger than the nature convection effect almost in any condition. When the enclosure number in width direction is increase to 5, and in length to 3, corresponding enclosure width 0.01160 m and length 0.06 m, the contribution of the nature convection to ETC has been less than 0.10% and can be ignored. The radiation effect ranges from 7.41% to 25.39% and cannot be ignored.

5.5. Temperature and velocity field for some typical cross-sections of concrete hollow bricks

Temperature and velocity distribution at cross-sections of two kinds of the concrete hollow bricks (B1-1 and B5-5) are shown in Figs. 10 and 11. Fig. 10 shows the temperature and velocity field at  $x = 0.12$  m for the brick B1-1. The plane at  $x = 0.012$  m is located at the enclosure center in length direction. Nature convection at this plane is strongest of all other sections.

Fig. 11 also illustrates the temperature and velocity vectors distribution of sectional plane at some enclosure center along  $x$  axis. From above figures, it can be observed from temperature field distribution that heat conduction becomes gradually predominant, which can be understood by parallel isothermals with increasing enclosure numbers in width direction. The distribution tendency for velocity field is also consistent with above viewpoint. The distorted distribution of isotherm implies intense nature convection and radiation. In fact, when enclosure number is increased to five in two directions, the nature convection and radiation become much weaker so that the further decrease of ETC becomes insignificant by increasing enclosure numbers afterwards. Therefore, much narrow enclosure widths of hollow bricks are not necessary

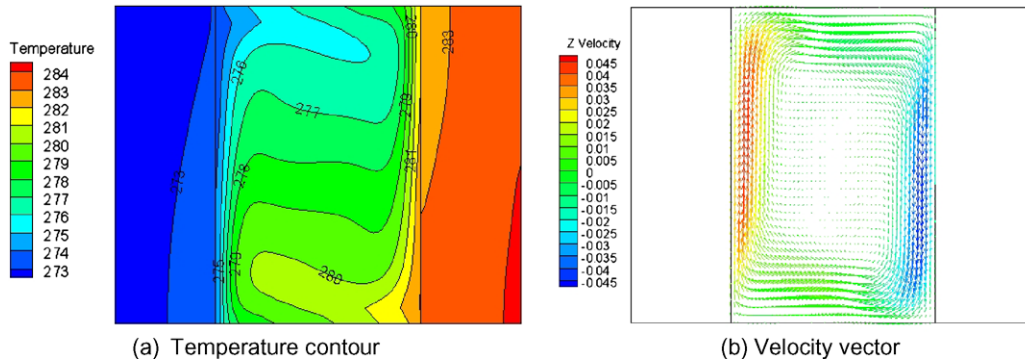


Fig. 10. Temperature and velocity field of the brick B1-1 at  $x = 0.12$  m.

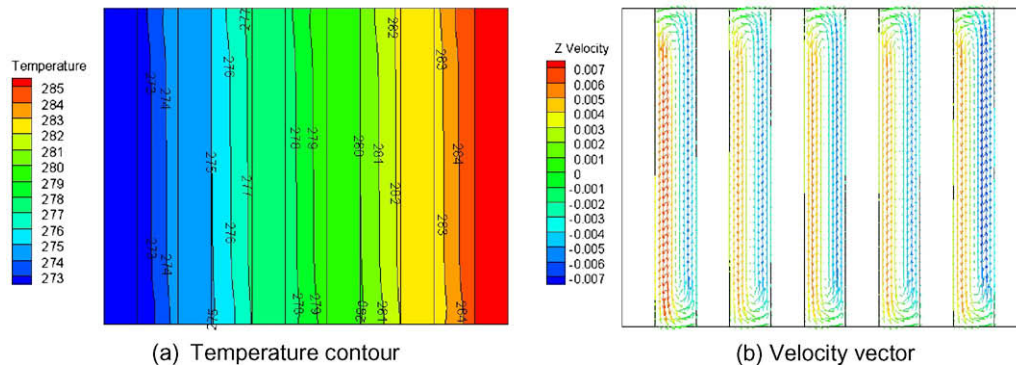


Fig. 11. Temperature and velocity field of the brick B5-5 at  $x = 0.12$  m.

for the improvement of energy saving when enclosure width reaches to 0.0116 m in the present research.

In the present paper, the optimum approach has not yet been introduced to the computing model. It is definitely important to get an optimum configuration with the minimum ETC. Besides, the transient boundary conditions will also have a sensitive influence on ETC, which is to be considered in future to understand the transient performance of the concrete hollow brick related to different season, latitude and altitude zone.

## 6. Conclusions

Numerical thermal analysis technique has been employed to study the heat transfer performance of 71 kinds of  $240 \times 115 \times 90$  concrete hollow bricks with various configurations. The configuration effect of concrete hollow brick on the equivalent thermal conductivity is inspected comprehensively. The conclusions are as follows:

- (1) ETC strongly depends on the combined effect of the heat conduction in concrete material, the natural convection within enclosure and the radiation on the inner surface. With increasing enclosure numbers in width direction, the natural convection and the surface radiation will be weakened as a result of increased thermal radiation shields and space limitation to the sufficient development of natural convection. With increasing enclosure numbers in length direction, ETC increases on contrary.
- (2) The relative enhancement of radiation heat transfer on ETC ranges from 7.41% to 25.39%, and the nature convection from 0.0049% to 22.50%, depending on the enclosure numbers and arrangement. The conduction effect is dominant in the present research. The radiation and nature convection should be instantly taken account during simulations when enclosure number is smaller than 5.
- (3) The influence of the enclosure staggered form on the heat transfer is strong, which can further decrease ETC from 11.59% to 20.94%, depending on the enclosure numbers.
- (4) When the thermal conductivity of concrete material is  $1.40 \text{ W}/(\text{m K})$ , the optimized ETC can reach  $0.32619 \text{ W}/(\text{m K})$  for brick S3-8 which can get energy saving of 23.30% related to solid concrete brick.

## Acknowledgements

Present authors express their gratefully acknowledgement for the financial support of this research by China University of Mining and Technology for the talent recruitment project. It is also grateful for Miss Min Li for her helpful prior work and for Miss Jing Han for his helps on diagram drawing at China University of Mining & Technology. It should also be mentioned here to thank ANSYS, Inc. for his reliable tool FLUENT® to give this research with reliable simulated results.

## References

- [1] Yang Dingyi, Sun Wei, Liu Zhiyong, Zheng Keren, Research on improving the heat insulation and preservation properties of small-size concrete hollow blocks, *Cement Concrete Res.* 33 (2003) 1357–1361.
- [2] J. Li, The effect of the hole types in the concrete hollow blocks on the heat insulation property, in: *The 1997 National Block Buildings' Design and Construction Technology Conference*, China Building Block Association Press, Yangzhou, 1997, pp. 261–266.
- [3] D.M. Kim, R. Viskanta, Heat transfer by conduction, natural convection and radiation across rectangular cellular structure, *Int. J. Heat Fluid Flow* 5 (1984) 205–212.
- [4] D.M. Kim, R. Viskanta, Effect of wall conduction and radiation on natural convection in a rectangular cavity, *Numer. Heat Transfer* 7 (1984) 449–470.
- [5] Ren Zepei, Zhang Lining, Jia Li, National convention in enclosure combined with conduction and radiation, *J. Eng. Thermophys.* 9 (3) (1988) 150–256.
- [6] J.F. Hinojosa, R.E. Cabanillas, G. Alvarez, C.E. Estrada, Nusselt number for the natural convection and surface thermal radiation in a square tilted open cavity, *Int. Commun. Heat Mass Transfer* 32 (2005) 1184–1192.
- [7] D. Misra, A. Sarkar, Finite element analysis of conjugate natural convection in a square enclosure with a conducting vertical wall, *Comput. Methods Appl. Mech. Eng.* 141 (1997) 205–219.
- [8] Moghtada Mobedi, Conjugate natural convection in a square cavity with finite thickness horizontal walls, *Int. Commun. Heat Mass Transfer* 35 (2008) 503–513.
- [9] C.Y. Zhao, W.Q. Tao, Natural convections in conjugated single and double enclosures, *Int. J. Heat Mass Transfer* 30 (1995) 175–182.
- [10] Majed M. Al-Hazmy, Analysis of coupled natural convection–conduction effects on the heat transport through hollow building blocks, *Energy Buildings* 38 (2006) 515–521.
- [11] J.J. del Coz Díaz, P.J. García Nieto, A. Martín Rodríguez, A. Lozano Martínez-Luengas, C. Betegón Biempica, Nonlinear thermal analysis of light concrete hollow brick walls by the finite element method and experimental validation, *Appl. Therm. Eng.* 26 (2006) 777–786.
- [12] J.J. del Coz Díaz, P.J. García Nieto, C. Betegón Biempica, M.B. Prendes Gero, Analysis and optimization of the heat-insulating light concrete hollow brick walls design by the finite element method, *Appl. Therm. Eng.* 27 (2007) 1445–1456.
- [13] J.J. del Coz Díaz, P.J. García Nieto, J.L. Suárez Sierra, C. Betegón Biempica, Nonlinear thermal optimization of external light concrete multi-enclosed brick walls by the finite element method, *Int. J. Heat Mass Transfer* 51 (2008) 1530–1541.
- [14] J.J. del Coz Díaz, P.J. García Nieto, J.L. Suárez Sierra, I. Peñuelas Sánchez, Non-linear thermal optimization and design improvement of a new internal light concrete multi-enclosed brick walls by FEM, *Appl. Therm. Eng.* 28 (2008) 1090–1100.
- [15] L.P. Li, Z.G. Wu, Y.L. He, G. Lauriat, W.Q. Tao, Optimization of the configuration of  $290 \times 40 \times 90$  hollow clay bricks with 3-D numerical simulation by finite volume method, *Energy Buildings* 40 (2008) 1790–1799.
- [16] L.P. Li, Z.G. Wu, Z.Y. Li, Y.L. He, W.Q. Tao, Numerical thermal optimization of the configuration of multi-holed clay bricks used for constructing building walls by the finite volume method, *Int. J. Heat Mass Transfer* 51 (2008) 3669–3682.
- [17] Yuan Zhang, Jiapeng He, Shouyun Gao, Research on heat resisting character of hollow building blocks in energy saving wall, *Envelope Technol. Building Energy Efficiency Vol. II-1–2* (2006).
- [18] D.D. Gray, A. Giorin, The validity of the Boussinesq approximation for liquids and gases, *Int. J. Heat Mass Transfer* 19 (1976) 545–551.
- [19] John H. Lienhard IV, John H. Lienhard V, *A Heat Transfer Textbook*, Cambridge, MA, 2005.
- [20] S.V. Patankar, *Numer. Heat Transfer Fluid Flow*, Hemisphere, Washington, DC, 1980.
- [21] M.G. Carvalho, T. Faris, P. Fontes, Predicting radiative heat transfer in absorbing, emitting, and scattering media using the discrete transfer method, in: W.A. Fiveland et al. (Eds.), *Fundamentals of Radiation Heat Transfer*, vol. 160 ASME HTD, 1991, pp. 17–26.
- [22] N.G. Shah, A New Method of Computation of Radiant Heat Transfer in Combustion Chambers, Ph.D. thesis, Imperial College of Science and Technology, London, England, 1979.